Analytical Solutions to Blocked Lubrication

Shuangbiao Liu (shuangbiaoliu@yahoo.com)
Tribo-Interface Design

Short Report

Keywords: Lubrication, Analytical solutions, Boundary conditions

Posted Date: May 6th, 2021

DOI: https://doi.org/10.21203/rs.3.rs-499984/v1

Analytical Solutions to Blocked Lubrication

Shuangbiao Liu

Tribo-Interface Design, 1309 Blue Sky Ct, Peachtree City, GA 30269

shuangbiaoliu@yahoo.com

Abstract

When mixed/boundary lubrication problems are studied, proper boundary conditions are needed to reflect the local physical reality that occurs between fluid lubrication and solid contacts. In order to improve understanding of such reality, often in a microscopic scale hidden from direct observation, simple lubrication problems with zero net exiting flow or blocked lubrication are identified, and several analytical solutions are derived for the first time based on one- and two-dimensional Reynolds equations.

Keywords: Lubrication; Analytical solutions; Boundary conditions

1. **Introduction**

Liu [1] summarizes various boundary conditions that are used together with the Reynolds equation in the full-film lubrication regime. Due to various design constrains, such as slow speed or heavy load, mixed lubrication or even boundary lubrication can occur in real life products. As a result, regions of solid contacts co-exist with regions of fluid lubrication, often in a microscopic scale hidden from direct observation. Solid contacts not only block flows but also reduce service life of these products and simulations if available are conducted in order to properly design such tribological interfaces. The sub-problem with regions of fluid lubrication is governed by the Reynolds equation together with additional boundary conditions reflecting local

physical reality of solid contact on one side and fluid lubrication on the other side. These additional boundary conditions are LCBCs in short.

Zhu and Wang [2] reviewed the history and progress of elastohydrodynamic lubrication (EHL) simulations, including lately significant accomplishments in relatively thin film deterministic solutions considering real measured roughness in the mixed and boundary lubrication regimes. Two approaches can be classified:

(1) On one hand, lubrication and solid-contact regions are treated separately with fluid-film pressure and dry-contact pressure variables, respectively, and these variables are updated in sequential sweeps of an iteration process. In 1995, Chang [3] studied transient mixed EHL line-contact problems with a deterministic model. His treatment of "check the film thickness at every grid point. If the film thickness is smaller than one-thousandth of the central film thickness for perfect smooth contact, h_{os}, set it to $0.001h_{os}$" allows the fluid-film pressure to be obtained from the Reynolds equation for the **entire** domain, therefore avoids the LCBCs. Then the solid-contact pressure is evaluated for grid points with negative gaps, which include deformations only caused by the fluid-film pressure. Results presented in [3] have non-zero fluid-film pressure values after the first (counting from the inlet) solid contact region, however this is physically impossible since lubricant should have been blocked by the first solid contact region and no fluid-film pressure should occur in the downstream after the solid contact. Jiang et al. [4] presented a transient mixed EHL model for point-contact problems. Their discretized Reynolds equation has three left-hand side terms involving three nodal pressures (triples) along the velocity direction and one right-hand term.

$$\alpha_{i,j}P_{i-1,j} + \beta_{i,j}P_{i,j} + \gamma_{i,j}P_{i+1,j} = b_{i,j}$$

Their treatments related to LCBCs can be summarized as following: when the film thickness at a node (i, j) is less than or equal to zero, (a) the film thickness is set to zero; (b) two coefficients, $\alpha_{i+1,j}$ and $\gamma_{i-1,j}$, need to be updated with zero film thickness; and (c) the fluid pressure is set to the solid-contact pressure.

Zhao et al. [5] simulated circular contacts start up, where the constraints (a) for the fluid-film lubrication regions are positive film thickness, zero solid-contact pressure, and non negative fluid-film pressure, (b) for the solid-contact regions are zero film thickness, positive solid-contact pressure, and zero fluid-film pressure. Deolalikar et al. [6] explicitly applied a no-flow boundary condition to boundaries where the fluid regions are upstream of the solid-contact regions.

(2) On the other hand, pressure variables, i.e., old and new pressure arrays during iterations, cover both lubrication and solid-contact regions, and are updated within the same sweep over nodes of an iteration process. Zhu and Hu [7] introduced a unified equation system, where

a) regular Reynolds equation for the lubrication regions,

b) truncated Reynolds equations--eliminating Poiseuille terms and a transient term, for solid-contact regions

Dimensionless film thickness is compared with a fixed small value to decide the truncation in (b). This approach is practical and has been successfully applied in their subsequent work [8]. Holmes et al. [9] used regular Reynolds equation and the elastic deflection equation in a differential form to update unknown nodal values of pressure and film thickness. Once a nodal value of film thickness is negative, it is set to zero and the nodal value of pressure is updated

with the elastic deflection equation only. Li and Kahraman [10], Azam et al. [11], and Wang et al. [12] utilized the unified equation system of Zhu and Hu [7].

The LCBCs in mixed/boundary EHL problems are microscopic, complex by nature, and often overlooked in experimental and fundamental studies, so it is important to understand/formulate them through focused investigations in order to enable physically meaningful numerical results. Given the situation, it is necessary to first address simpler lubrication problems under simpler configurations. In this paper, several analytical solutions are derived for the first time based on one- or two-dimensional Reynolds equations without net exiting lubricant—blocked lubrication problems. These solutions themselves may be applicable to special engineering problems or to be used to validate numerical algorithms in the mixed/boundary lubrication study. Also, they can be exercises for students in the tribology field, and can help readers to better understand lubrication where flow is blocked locally. In the future work, reasonable boundary conditions can be introduced to deal with boundaries between fluid lubrication and solid contacts, and they ultimately allow details closer to reality around solid contacts to be obtained in lubrication simulations.

2. Analytical Solutions

In the following steady-state lubrication problems, flow through the lubrication area is intentionally blocked in one direction, in order to gain insights of film pressure involving solid contacts in mixed lubrication. They are mostly two dimensional problems, but one three dimensional pad bearing problem is also analytically solved in section 2.5.

For simplicity, density ρ are constant. Also in sections 2.1 to 2.3, and 2.5, lubricant viscosity η is constant and bodies are rigid. In section 2.4, the Barus viscosity-pressure

relationship is used with an elastic cylinder. Furthermore, referring to Figs. 1-5, it is assumed that (a) The bottom plate is always flat and horizontal moving along the x axis with a constant velocity of u, and the top plate is stationary with various shapes; (b) no air has been trapped inside for all problems; (c) a perfect sealing exists between the rigid block plate and the moving plate, and (d) there is no slip between lubricant and the plate surfaces. One could use this website https://www.wolframalpha.com/ or softwares such as mathematica® or Maple ® to help derivation.

2.1 Straight plate

Problem 1 has a tilted straight plate and a block plate, both of which are rigid surfaces (see Fig. 1). The gap in the inlet is h_i and the gap on the blocked side is h_0.

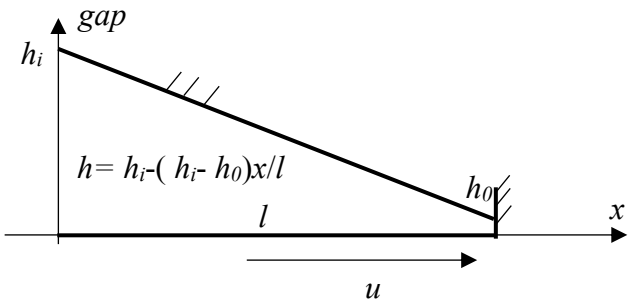

Fig. 1 Tilted straight plate, blocked exit

When steady state cases are considered, the one-dimensional Reynolds equation is written as

$$\frac{d}{dx}\left(\frac{\rho h^3}{\eta}\frac{dp}{dx}\right) = 6u\frac{d(\rho h)}{dx} \tag{1}$$

After an integration, one can find,

$$\frac{h^3}{\eta}\frac{dp}{dx} = 6uh + C \tag{2}$$

Integration constant C can be determined with the fact of no flow through the region. Flow is defined as

$$q = -\frac{h^3}{12\eta}\frac{dp}{dx} + \frac{uh}{2} = 0 \tag{3}$$

so apparently, C = 0. Then one has this important equation

$$\frac{h^3}{\eta}\frac{dp}{dx} = 6uh \tag{4}$$

After substituting the film shape and another integration,

$$\frac{p}{\eta u} = \frac{6l}{h_i(h_i - h_0)}\left[\frac{h_i l}{h_i l - (h_i - h_0)x} + D\right] \tag{5}$$

Integration constant D is determined by inlet boundary condition: $p = 0$ at $x = 0$, so $D = -1$. After simplification, the solution of p is obtained as,

$$\frac{p}{\eta u} = \frac{6l}{h_i}\frac{x}{h_i l - (h_i - h_0)x} = \frac{6}{h_i}\frac{x}{h} \tag{6}$$

So the pressure is a linear function of x and the inverse of gap h. At the right end, $x = l$, the pressure is

$$\frac{p}{\eta u} = \frac{6l}{h_i h_0} \tag{7}$$

When h_0 is close to zero, the pressure there becomes very large. However, in reality the situation with near-zero h_0 at the blocked exit is very complicated and some of assumptions mentioned above may not be valid anymore. Thus, it is beyond the scope of this work. Note that if the top

plate is parallel to the bottom one, there is still pressure build up and the pressure distribution is a linear function of x.

2.2 Plate with a step

Figure 2 shows a tilted plate with an interior step, where the gap value changes from h_0 to h_1. Equation (4) is applicable for both regions separated by the step. For the left region, the result in section 2.1 is still valid. For the right region, the film shape is

$$h = h_1 - \frac{(h_1-h_2)(x-l)}{l_1} \tag{8}$$

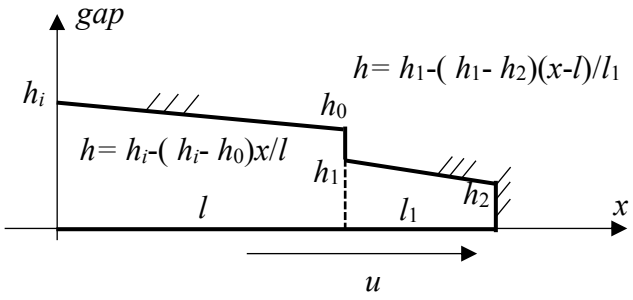

Fig. 2 Tilted plate with a step, blocked exit

After substituting the film shape into Eq. (4) and an integration,

$$\frac{p}{\eta u} = \frac{6l_1}{h_1(h_1-h_2)}\left(\frac{1}{1-\frac{(h_1-h_2)(x-l)}{h_1 l_1}} + D_2\right) \tag{9}$$

Integration constants D_2 should be determined by pressure continuity at $x = l$. One can find

$$\frac{6\eta u l_1}{h_1(h_1-h_2)}(1 + D_2) = \frac{6\eta u l}{h_i h_0} \tag{10}$$

So,

$$D_2 = \frac{l(h_1-h_2)h_1}{l_1 h_i h_0} - 1 \tag{11}$$

In summary,

$$\frac{p}{\eta u}=\begin{cases}\frac{6l}{h_i}\frac{x}{h_i l-(h_i-h_0)x} & x\le l\\ \frac{6l_1}{h_1}\left(\frac{x-l}{h_1 l_1-(h_1-h_2)(x-l)}+\frac{lh_1}{l_1 h_i h_0}\right) & x>l\end{cases} \tag{12}$$

If h_1 equals to h_0, step disappears, this plate has a point, and this solution is still valid.

2.3 Cylinder

This problem involves a rigid cylinder with a radius of R. The minimum gap is h_0, and the block plate is at $x = x_0$, see Fig. 3. The film shape is

$$h=h_0+\frac{x^2}{2R} \tag{13}$$

After substituting the film shape into Eq. (4) and an integration,

$$\frac{p}{\eta u}=\frac{3}{h_0^2}\left[\frac{x}{1+\frac{x^2}{2Rh_0}}+\omega\,\mathrm{atan}\left(\frac{x}{\omega}\right)+D\right] \tag{14}$$

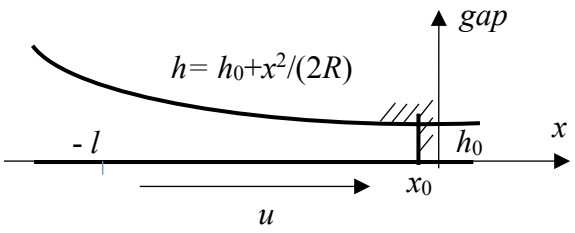

Fig. 3 Cylinder, blocked exit

Where $\omega=\sqrt{2Rh_0}$. Integration constant D is determined by inlet boundary condition: $p = 0$ at $x = -l$, so

$$D=\frac{l}{1+\frac{l^2}{2Rh_0}}+\omega\,\mathrm{atan}\left(\frac{l}{\omega}\right) \tag{15}$$

After simplification, the solution of p is obtained as,

$$\frac{p}{\eta u} = \frac{3}{h_0^2}\left[\frac{x+l}{1+\frac{x^2}{2Rh_0}} + \omega \operatorname{atan}\left(\frac{x}{\omega}\right) + \omega \operatorname{atan}\left(\frac{l}{\omega}\right)\right] \tag{16}$$

One can see this solution does not contain x_0. If x_0 is negative, it has a convergent geometry, so this solution is valid for the entire length of l. But if x_0 is positive, the portion beyond $x = 0$ is divergent. Even in this divergent gap, this solution is valid. When $x_0 = 0$, pressure reaches this value

$$\frac{p}{\eta u} = \frac{3}{h_0^2}\left[l + \omega \operatorname{atan}\left(\frac{l}{\omega}\right)\right] \tag{17}$$

2.4 Simplified EHL

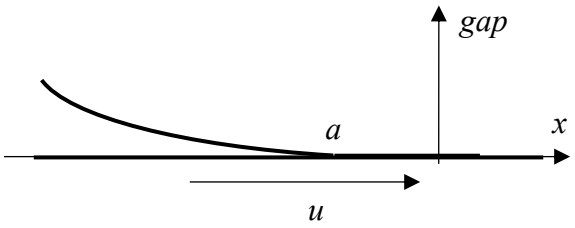

Fig. 4a Deformed cylinder

Section 10.4 (C) in Johnson's book [13] (also in Morales-Espejel et al., [14]) discussed the EHL inlet analyses with the Barus viscosity-pressure relationship,

$$\eta = \eta_o \exp(\alpha p) \tag{18}$$

The reduced pressure

$$p' = [1 - \exp(-\alpha p)]/\alpha \tag{19}$$

is applied.

Figure 4a illustrates an elastic cylinder (radius of R) and a rigid plate under a load. The Hertzian contact width is a. dimensionless coordinate X is defined as x/a. **Without considering the deformation from the fluid pressure**, the gap between these two bodies when $X \leq -1$ can be expressed as,

$$h = \frac{a^2}{2R}\left[-X\sqrt{X^2-1} - \ln\left(-X + \sqrt{X^2-1}\right)\right] \tag{20}$$

In order to facilitate integration, Eq. (20) can be approximated as follows, see Eq. (10.38) of [13],

$$\text{Appr. 1:} \qquad h \approx \frac{a^2}{3R}[-2(X+1)]^{1.5} \tag{21}$$

It is found that this approximation is reasonable for $-1.5 \leq X \leq -1$ and the exponent of 1.673 has much better approximation for $-4 \leq X \leq -1.5$,

$$\text{Appr. 2:} \qquad h \approx \frac{a^2}{3R}[-2(X+1)]^{1.673} \tag{22}$$

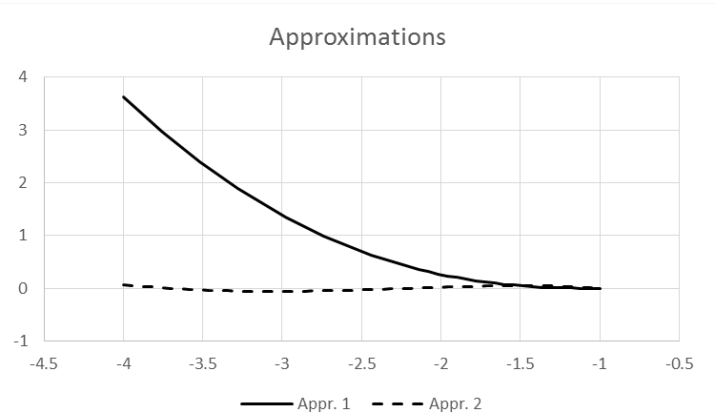

Fig. 4b Absolute errors from two approximations of $2R\ h/a^2$: with exponents of 1.5 (Solid line) and 1.673 (Dashed-line)

Absolute errors from these two approximations of $2R\ h/a^2$ are compared in Fig. 4b. Solid line represents $-X\sqrt{X^2-1}-\ln\left(-X+\sqrt{X^2-1}\right)-\frac{2}{3}[-2(X+1)]^{1.5}$, and the dashed line is $-X\sqrt{X^2-1}-\ln\left(-X+\sqrt{X^2-1}\right)-\frac{2}{3}[-2(X+1)]^{1.673}$, which has much less absolute error when $X \leq -1.5$.

Substituting Eqs. (21-22) into Eq. (4) gives,

$$\frac{dp\prime}{dX}=\frac{6au\eta_0}{h^2} \tag{23}$$

After integration with the film shape of Eq. (21), one can obtain

$$\frac{dp\prime}{dX}=\frac{54u\eta_0R^2}{a^3}\frac{1}{[2(X+1)]^{3.346}}=\frac{5.31u\eta_0R^2}{a^3}\frac{1}{(X+1)^{3.346}} \tag{24a}$$

$$p'=\frac{2.26u\eta_0R^2}{a^3}\left(\frac{1}{(-X-1)^{2.346}}+D\right) \tag{24b}$$

The integration constant D is determined by the inlet boundary condition of $p'=0$ at $X=-4$, so $D=-\frac{1}{3^{2.346}}$. Therefore the reduced pressure for $-4 \leq X \leq -1.5$ is

$$p'=\frac{2.26u\eta_0R^2}{a^3}\left(\frac{1}{(-X-1)^{2.346}}-\frac{1}{3^{2.346}}\right) \tag{25}$$

For $-1.5 \leq X \leq -1$, similarly derivation but with Eq. (22) gives,

$$\frac{dp\prime}{dX}=\frac{54u\eta_0R^2}{a^3}\frac{1}{[2(X+1)]^3}=\frac{27uR^2}{4a^3}\frac{1}{(X+1)^3} \tag{26a}$$

$$p'=\frac{27u\eta_0R^2}{8a^3}\left(\frac{1}{(X+1)^2}+D_1\right) \tag{26b}$$

Using pressure continuity at $X=-1.5$, the constant D_1 can be determined,

$$D_1=\frac{2.26}{3.375}\left(\frac{1}{(0.5)^{2.346}}-\frac{1}{3^{2.346}}\right)-4 \approx -0.6464$$

Therefore, the reduced pressure for $-1.5 \le X \le -1$ is

$$p' = \frac{27u\eta_0 R^2}{8a^3}\left(\frac{1}{(X+1)^2} - 0.6464\right) \tag{27}$$

The pressure can be found from

$$p = -\frac{\ln(1-\alpha p')}{\alpha} \tag{28}$$

Example: the value of α is 2.28E-8, R is 20mm, a is 0.1mm, u is 100mm/s, $\eta_0 = 0.04247$ Pa.s.

a) If the maximum pressure inside this wedge is 1E6 Pa,

p'=[1 − exp(−αp)]/α =988686

This pressure is in the region of $-4 \le X \le -1.5$,

$\frac{1}{3^{2.346}} + p'\frac{a^3}{2.26u\eta_0 R^2} = 0.333$ and $X = -0.333^{-\frac{1}{2.346}} - 1 = -2.597$

X is -2.597.

b) If X is given, one can find the pressure value there. When $X = -1.35$,

$$p' = \frac{27u\eta_0 R^2}{8a^3}\left(\frac{1}{(X+1)^2} - 0.6464\right) = 43097571$$

And $p = -\frac{\ln(1-\alpha p')}{\alpha} = 0.1778$E9 Pa

Beyond this location, the pressure increases dramatically. Note that when the speed is slower, X needs to be closer to −1 to reach the same pressure value. If the deformation from the fluid pressure has to be considered in the calculation, one has to use numerical simulations.

2.5 Fixed incline pad bearing blocked at the exit

Figure 5 shows a fixed incline pad bearing with a blocked exit. This is a three-dimensional lubrication problem and requires a two-dimensional Reynolds' equation.

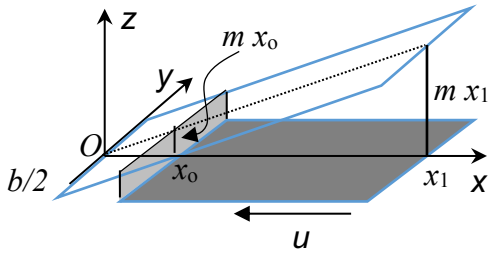

Figure 5 Fixed incline pad bearing, blocked exit

$$\frac{\partial}{\partial x}\left(\frac{h^3}{\eta}\frac{\partial p}{\partial x}\right)+\frac{\partial}{\partial y}\left(\frac{h^3}{\eta}\frac{\partial p}{\partial y}\right)=-6u\frac{\partial h}{\partial x} \tag{29}$$

where

$$h = mx$$

and m is the slope. For simplicity, the dimensionless pressure is introduced as,

$$P=\frac{m^2 p}{\eta u} \tag{30}$$

And the Reynolds equation is expressed as,

$$\frac{\partial^2 P}{\partial x^2}+\frac{\partial^2 P}{\partial y^2}+\frac{3}{x}\frac{\partial P}{\partial x}+\frac{6}{x^3}=0 \tag{31}$$

For the problem of a rectangular pad without any blockage, Michell [15] is the genius who presented a novel solution, and 35 years later, Muskat et al. [16] constructed another type of solution. With more derivation details, Hays [17] reached slightly complicated expressions than

what is in Muskat et al. [16]. Liu and Mou [18] derived a general solution which unifies these two existing groups of analytical solutions, and also showed that Hays' solution is actually equivalent to what Muskat et al. derived. The core idea in the work of Muskat et al. [16] and Hay [17] is that the solution for an *infinite* sliding pad can eliminate the inhomogeneity of Eq. (29), then the separation of variable can be used to solve the homogenous PDE. The solution for an infinite sliding pad, Eq. (6), is the corresponding particular solution, and will be re-written based on notations in Fig. 5 as,

$$P = \frac{6}{x_1}\frac{x_1 - x}{x} \tag{32}$$

which satisfies the 1D Reynolds equation of $\frac{\partial^2 P}{\partial x^2} + \frac{3}{x}\frac{\partial P}{\partial x} + \frac{6}{x^3} = 0$. Therefore, the homogenous equation becomes,

$$\frac{\partial^2 P}{\partial x^2} + \frac{\partial^2 P}{\partial y^2} + \frac{3}{x}\frac{\partial P}{\partial x} = 0 \tag{33}$$

One can use separation of variables, and obtain the general solution to the homogenous equation, which is a linear combination of all possible solutions [18],

$$P = (c_1 + c_2 y)\left(d_1 + \frac{d_2}{x^2}\right) + \tag{34}$$

$$\sum_{n=0}^{\infty}[c_{1n}\sinh(\alpha_{1n}y) + c_{2n}\cosh(\alpha_{1n}y)][d_{1n}J_1(\alpha_{1n}x) + d_{2n}Y_1(\alpha_{1n}x)]\frac{1}{\alpha_{1n}x} +$$

$$\sum_{n=0}^{\infty}[c_{3n}\sinh(\alpha_{2n}y) + c_{4n}\cosh(\alpha_{2n}y)][d_{3n}I_1(\alpha_{2n}x) + d_{4n}K_1(\alpha_{2n}x)]\frac{1}{\alpha_{2n}x}$$

where $J_1(z)$ and $Y_1(z)$ are the Bessel functions of the first and second kinds, respectively, and $I_1(z)$ and $K_1(z)$ are the *modified* Bessel functions of the first and second kinds, respectively. By

selecting their proper values of unknown constants c_j, d_j, c_{in}, d_{in}, and α_{jn} (i =1…4, j =1 or 2), one should be able to solve problems with complicated boundary conditions.

Following Muskat et al. [16] and Hay [17] successes, the middle line of Eq. (34) with Bessel functions will be selected for the problem in Fig. 5, and

$$U_n(x) = J_1(\alpha_n x_1)Y_1(\alpha_n x) - Y_1(\alpha_n x_1)J_1(\alpha_n x) \tag{35}$$

is defined with x_1 the inlet coordinate to satisfy zero pressure boundary condition at x_1 since $U_n(x_1) = 0$. α_n is used to replace α_{1n} for simplicity. The origin of the coordinate system in Fig. 5 was deliberately set in the middle of width, so the two boundary conditions are at $y = \pm b/2$ and terms with the "Cosh" function are suitable and selected,

$$P = \frac{6}{x_1}\frac{x_1 - x}{x} + \sum_{n=1}^{\infty} \frac{6U_n(x)}{x}\frac{C_n \cosh(\alpha_n y)}{\cosh(\alpha_n b/2)} \tag{36}$$

C_n is used to replace C_{1n} for simplicity. The solution for an infinite sliding pad with a blocked exit is the corresponding particular solution and is the first term in Eq. (36). The coefficient, α_n will be determined with the exit boundary condition. Flow equation is expressed as

$$\frac{q}{um} = -\frac{x}{2} - \frac{x^3}{12}\frac{\partial P}{\partial x} \tag{37}$$

The derivative involved in the above expression is quite complicate, so a new function is defined as

$$W_n(x) = J_1(\alpha_n x_1)Y_2(\alpha_n x) - Y_1(\alpha_n x_1)J_2(\alpha_n x) \tag{38}$$

to satisfy the following derivative,

$$\frac{\partial}{\partial x}\left[\frac{U_n(x)}{x}\right] = -\frac{\alpha_n W_n(x)}{x}$$

Thus,

$$\frac{\partial P}{\partial x} = \frac{\partial}{\partial x}\left[\frac{6}{x_1}\frac{x_1 - x}{x} + \sum_{n=1}^{\infty}\frac{6U_n(x)}{x}\frac{C_n\cosh(\alpha_n y)}{\cosh(\alpha_n b/2)}\right]$$

$$= -\frac{6}{x^2} - \sum_{n=1}^{\infty}\frac{6\alpha_n W_n(x)}{x}\frac{C_n\cosh(\alpha_n y)}{\cosh(\alpha_n b/2)}$$

At the exit, x_0, flow is blocked, so

$$\left[-\frac{x}{2} - \frac{x^3}{12}\frac{\partial P}{\partial x}\right]\Big|_{x_0} = 0$$

One can obtain

$$W_n(x_0) = 0 \tag{39a}$$

Or

$$J_1(\alpha_n x_1)Y_2(\alpha_n x_0) - Y_1(\alpha_n x_1)J_2(\alpha_n x_0) = 0 \tag{39b}$$

This equation is used to calculate the coefficient, α_n. Based on the recurrence relations in the Appendix, the Bessel functions of the order of 2 can be expressed with those of lower orders. So, one can have the following form,

$$J_1(\alpha_n x_1)[2Y_1(\alpha_n x_0) - \alpha_n x_0 Y_0(\alpha_n x_0)] - Y_1(\alpha_n x_1)[2J_1(\alpha_n x_0) - \alpha_n x_0 J_0(\alpha_n x_0)] = 0 \tag{39c}$$

Introducing two general variables,

$$\tau = x_1/x_0$$

$$\beta_n = \alpha_n x_0$$

The equation is simplified as

$$J_1(\beta_n\tau)Y_2(\beta_n) - Y_1(\beta_n\tau)J_2(\beta_n) = 0 \tag{40}$$

One can see that β_n is solely dependent on the variable τ. The coefficients, α_n, can then be easily obtained from β_n, i.e., β_n/x_0. This equation (39c) is also used in the Appendix to simplify formulae that are used to determine the other coefficients, C_n.

The remaining boundary conditions are on the two sides, i.e. $P\left(x,\frac{b}{2}\right)=0$, and one has

$$0 = 1 - \frac{x}{x_1} + \sum_{n=1}^{\infty} C_n U_n(x) \tag{41}$$

One can use this equation and the orthogonality of U_n (see Appendix) to determine the coefficients, C_n. The method is to multiply $xU_m(x)$ for every term on both sides and then integrate with respect to x from x_0 to x_1. Due to orthogonality of U_n, terms with $n \neq m$ inside the summation are zero, and only one term with $n = m$ inside the summation is non-zero (see Appendix). Denote $S_{amb} = S_a(\alpha_m x_b)$ where S can be J, Y, or H (the Struve function), and a and b could be 0, 1, or 2. For example, $J_{1n1} = J_1(\alpha_n x_1)$ or $H_{0n0} = H_0(\alpha_n x_0)$. All integrations are discussed in the Appendix. After simplification, one can found the coefficients of C_n from Eqs. (A13-A14) as,

$$C_n = \frac{H_{1n1} + \frac{\pi}{2}\Delta(\alpha_n x_0 H_{0n0} - 2H_{1n0}) + \frac{2}{\pi}}{\frac{2}{\pi^2} - \frac{(\alpha_n x_0 \Delta)^2}{2}} = \frac{2\pi^2 H_{1n1} + \pi^3 \Delta(\alpha_n x_0 H_{0n0} - 2H_{1n0}) + 4\pi}{4 - (\pi \alpha_n x_0 \Delta)^2} \tag{42}$$

Where H_ν are the Struve function of order ν and $\Delta = J_{1n1}Y_{1n0} - Y_{1n1}J_{1n0} = U_n(x_0)$. Note that both sets of coefficients, α_n and C_n, are determined without involving the width, b. In other words, problems with different widths can use the same sets of these coefficients.

3. Results and discussion

For the problem in section 2.1, one example is described as: the length of 30mm, inlet gap of 1mm, and the exit gap of 0.4mm, i.e., l = 30mm, h_i = 1mm, and h_0 = 0.4mm. The modified pressure ($\frac{p}{\eta u}$) and gap distributions are shown in Fig. 6 with a label of "line". For the problem in section 2.2, the step is 20mm away from the inlet and the heights are 0.7 and 0.5mm, The modified pressure and gap distributions are shown in Fig. 6 with a label of "step". The last case shown in Fig. 6 with a label of "bent" is for a bent plate with the minimum gap of 0.35mm. One can see there are pressure further built-up inside the divergent gap.

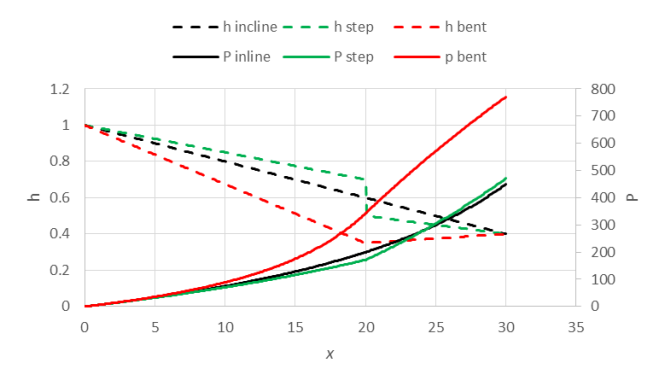

Fig. 6 Three plates and their modified pressure

The example for section 2.3 has a radius R of 20mm, l = 2mm, and h_0 = 0.05mm. So $\omega = \sqrt{2Rh_0}=\sqrt{2}$. Figure 7 shows the gap and the modified pressure.

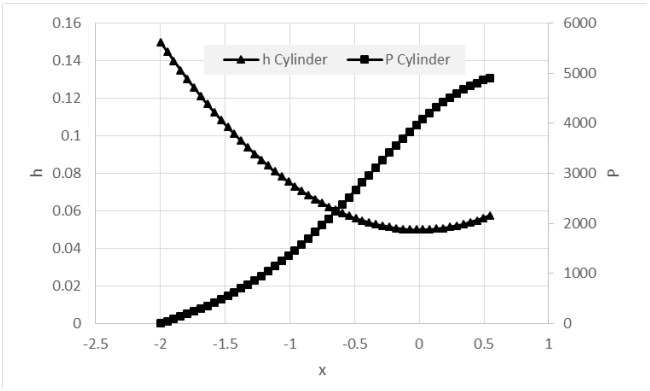

Fig. 7 Cylinder and its modified pressure

For the 3D problem in section 2.5, the parameters l = 30mm, h_i = 1mm, and h_0 = 0.4mm are also used. Thus, the coordinates of x_0 and x_1 are 20 and 50 mm, respectively. m = 0.02 and $\tau = \frac{x_1}{x_0} = 2.5$. In addition, two widths of the plate are used 20 and 40 mm, i.e., b = 10 and 20mm, respectively. The solutions of Eq. (45),

$$J_1(\beta_n\tau)Y_2(\beta_n) - Y_1(\beta_n\tau)J_2(\beta_n) = 0$$

can be determined by a FORTRAN program or through https://www.wolframalpha.com/ with the input of,

solve(BesselY(2, x)*BesselJ(1, 2.5*x) - BesselJ(2, x)*BesselY(1, 2.5*x) =0 , x=0 to 20)

and the first 9 positive roots are listed in Table 1. The coefficients of $\alpha_n = \beta_n/x_0$ can be readily obtained. The same website can calculate the corresponding values of the Struve functions, which are also listed in Table 1. The values of Δ, Bessel functions, and the coefficients, C_n are listed in Table 2.

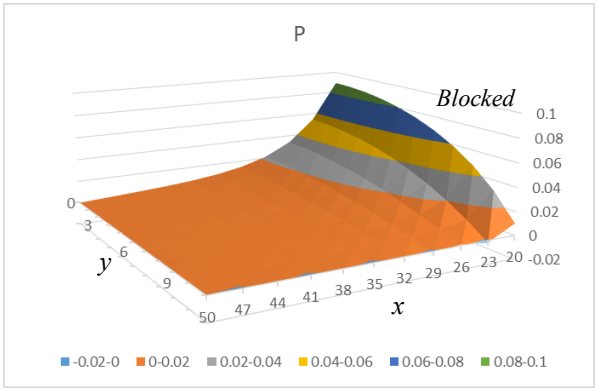

Fig. 8 Distribution of the modified pressure shown with y from 0 to 10.

With 9 terms of summation in Eq. (41), the distribution of modified pressure for the case with the width of 20mm are obtained for half of the width due to symmetry, and is shown in Fig. 8. In Fig. 9, a comparison is shown, where "1d" is for the infinite width, "2d 40" is for the centerline pressure distribution with the width of 40mm, and "2d" is for the centerline pressure distribution with the width of 20mm. One can see the narrower the width, the less pressure build-up. The label "edge" is for the pressure on the edge of the plate with the width of 20mm, all of which should be zero. However, one can see numerical errors exist, particularly when x is around 20. Double precision and more summation terms can reduce such errors.

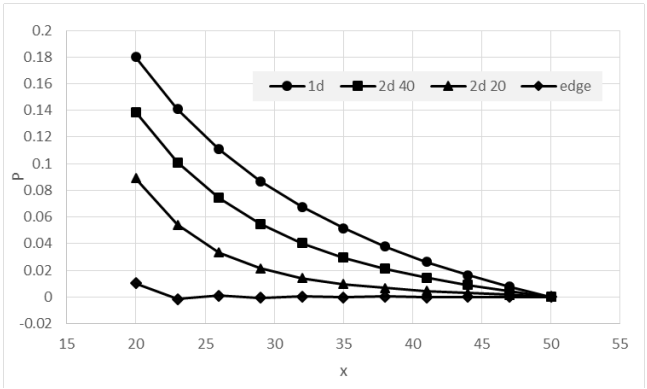

Fig. 9 Comparison of modified pressure

Solutions of pressure, particularly around the centerline, can be used to validate the boundary condition treatment of numerical algorithms in the mixed lubrication.

4. Conclusions

Several analytical solutions to lubrication problems with blocked exits have been derived. They are critical to understand the boundary conditions between solid contact and fluid lubrication occurring in the mixed/boundary lubrication regimes.

Acknowledgements

The author would acknowledge his family's financial support during COVID-19, which make this work possible.

Funding

This research did not receive any specific grant from funding agencies in the public, commercial, or not-for-profit sectors.

Nomenclature

a = Hertzian contact width in section 2.4 (m)

b = width of the plate in section 2.5 (m)

C, D = integration constants

h = film thickness (m)

h_0, h_i, h_1, h_2 = gaps (m)

q = mass flow per unit length (kg/m/s)

p = pressure (Pa)

$P = \frac{m^2 p}{\eta u}$, modified pressure in section 2.5

R = radius (m)

l, l_1 = length of a lubrication region (m)

m = slope

u = horizontal velocity of the bottom plate along the x axis (m/s)

F = total force per length (N/m)

x , X = coordinate (m) and its dimensionless value, $X = x/a$ in section 2.4

x_0 , x_1 = coordinate (m) in section 2.5

α = pressure-viscosity coefficient (Pa^{-1})

α_i, β_i, γ_i, δ_i = coefficients and right-hand side in the discrete Reynolds equation

α_n, β_n, C_n = coefficients in the solution of pressure

η = viscosity (Pa·s)

η_0 = viscosity at atmospheric pressure (Pa·s)

ρ = density (kg/m^3)

$$\Delta = J_{1n1}Y_{1n0} - Y_{1n1}J_{1n0} = J_1(\alpha_n x_1)Y_1(\alpha_n x_0) - Y_1(\alpha_n x_1)J_1(\alpha_n x_0)$$

$$\tau = x_1/x_0$$

References

[1] Liu S. On Boundary Conditions in Lubrication with One Dimensional Analytical Solutions. Tribol Int 2012;48:182–190.

[2] Zhu D, Wang Q. Elastohydrodynamic Lubrication: A Gateway to Interfacial Mechanics - Review and Prospect. J Tribol 2011;133(4):041001.

[3] Chang L. A Deterministic Model for Line Contact Partial Elastohydrodynamic Lubrication. Tribol Int 1995;28:75–84.

[4] Jiang X, Hua DY, Cheng HS, Ai X, Lee SC. A Mixed Elastohydrodynamic Lubrication Model with Asperity Contact. J Tribol 1999;121:481–491.

[5] Zhao JX, Sadeghi F, Hoeprich MH. Analysis of EHL Circular Contact Start Up: Part I—Mixed Contact Model with Pressure and Film Thickness Results. J Tribol 2001;123:67–74.

[6] Deolalikar N, Sadeghi F, Marble S. Numerical Modeling of Mixed Lubrication and Flash Temperature in EHL Elliptical Contacts. J Tribol 2008;130:011004-1.

[7] Zhu D, Hu YZ. The Study of Transition from Full Film Elastohydrodynamic to Mixed and Boundary Lubrication. The Advancing Frontier of Engineering Tribology, Proceedings of the 1999 STLE/ASME H.S. Cheng Tribology Surveillance:150–156.

[8] Hu YZ, Zhu D. A Full Numerical Solution to the Mixed Lubrication in Point Contacts. J Tribol 2000;122:1-9.

[9] Holmes MJA, Evans HP, Snidle, RW. Analysis of Mixed Lubrication Effects in Simulated Gear Tooth Contacts. J Tribol 2005;127:61–69.

[10] Li S, Kahraman A. A Mixed EHL Model with Asymmetric Integrated Control Volume Discretization. Tribol Int 2009;42:1163–1172.

[11] Azam A, Dorgham A, Morina A, Neville A, Wilson M. A simple deterministic plastoelastohydrodynamic lubrication (PEHL) model in mixed lubrication. Tribol Int 2019;131:520-529.

[12] Wang Y, Dorgham A, Liu Y, Wang C, Wilson M, Neville A, Azam A. An Assessment of Quantitative Predictions of Deterministic Mixed Lubrication Solvers. J. Tribol, 2021;143(1): 011601.

[13] Johnson KL. *Contact Mechanics*. Cambridge University Press; 1987.

[14] Morales-Espejel GE, Dumont ML, Lugt PM, Olver AV. A Limiting Solution for the Dependence of Film Thickness on Velocity in EHL Contacts with Very Thin Films. Tribol Transactions 2005;48(3):317-327.

[15] Michell AGM. Lubrication of Plane Surfaces. Zeitschrift für Mathematik und Physik, 1905 (Transactions of the Institution of Engineers 1988;**12** (3-4):48-62).

[16] Muskat M, Morgan F, Meres MW. The Lubrication of Plane Sliders of Finite Width. J Applied Physics. 1940;**11**:208-219.

[17] Hays DF. Plane Sliders of Finite Width. Tribol Transactions, 1958;**1** (2):233-240.

[18] Liu S, Mou L. Hydrodynamic Lubrication of Thrust Bearings with Rectangular Fixed-Incline-Pads. J Tribol, 2012;134 (2):024503

Appendix

A.1 Recurrence relations of Bessel functions

J_n and Y_n are the Bessel functions of the first and second kinds, respectively. n is the order. If S is a representative symbol for these Bessel functions, either J_n or Y_n but no mixing, one has the following relationship,

$$S_{n+1}(z)+S_{n-1}(z) = \frac{2nS_n(z)}{z} \tag{A.1}$$

For instance, if $n = 1$, it is true that

$$S_2(z)+S_0(z) = \frac{2S_1(z)}{z} \tag{A.2}$$

One can verify that

$$J_1(z)Y_0(z) - J_0(z)Y_1(z) = \frac{2}{\pi z} \tag{A.3}$$

A.2 Integrals related to Bessel functions

Integrations of multiplications among x and two of these Bessel functions of the first and second kinds, $S_1(x)$ and $T_1(x)$ which can be either $J_1(x)$ or $Y_1(x)$, are as follows,

$$2\int S_1(x)T_1(x)xdx = x^2[S_0(x)T_0(x) + S_1(x)T_1(x)] - 2xS_1(x)T_0(x) \tag{A.4}$$

Note if S and T are different functions, the last term can have 2 equivalent options, $S_1(x)T_0(x)$ or $S_0(x)T_1(x)$.

Also, integrations of multiplications among x and two of these Bessel functions of the first and second kinds with **different variables** are as follows,

$$(a^2-1)\int S_1(x)T_1(ax)xdx = x[S_0(x)T_1(ax) - aS_1(x)T_0(ax)] \tag{A.5}$$

Furthermore,

$$2\int S_1(x)xdx = \pi x[H_0(x)S_1(x) - H_1(x)S_0(x)] \tag{A.6}$$

$$\int S_1(x)x^2dx = x^2S_2(x) = -x^2S_0(x) + 2xS_1(x) \tag{A.7}$$

A.3 Orthogonality of U_n

The definition of $\boldsymbol{U_n}$ is given in Eq. (40),

$$U_n(x) = J_1(\alpha_n x_1)Y_1(\alpha_n x) - Y_1(\alpha_n x_1)J_1(\alpha_n x)$$

Denote $S_{acb} = S_a(\alpha_c x_b)$ where S can be J and Y, c can be m and n, and a and b are integers, e.g., $J_{1m1} = J_1(\alpha_m x_1)$. The following integrations are of interest,

$$\int_{x_0}^{x_1} xU_m(x)U_n(x)dx$$

$$= \frac{1}{\alpha_m^2}\int_{\alpha_m x_0}^{\alpha_m x_1} z[J_{1m1}Y_1(z) - Y_{1m1}J_1(z)][J_{1n1}Y_1(az) - Y_{1n1}J_1(az)]dz \tag{A.8}$$

where $z = \alpha_m x$, $a = \alpha_n/\alpha_m$.

a. When $m \neq n$, one can easily use the above integrals, Eq. (A.5) to obtain that

$$\alpha_m^2(a^2-1)\int_{x_0}^{x_1} xU_m(x)U_n(x)dx$$

$$= \{J_{1m1}J_{1n1}[zY_0(z)Y_1(az) - azY_1(z)Y_0(az)]$$

$$+Y_{1m1}Y_{1n1}[zJ_0(z)J_1(az) - azJ_1(z)J_0(az)]$$

$$-J_{1m1}Y_{1n1}[zY_0(z)J_1(az) - azY_1(z)J_0(az)]$$

$$-Y_{1m1}J_{1n1}[zJ_0(z)Y_1(az) - azJ_1(z)Y_0(az)]\}|_{\alpha_m x_0}^{\alpha_m x_1} \equiv 0 \quad \text{(A.9)}$$

During derivation, boundary conditions at x_0 need to be used with α_n and α_m:

$$J_{1n1}[2Y_{1n0} - \alpha_n x_0 Y_{0no}] - Y_{1n1}[2J_{1n0} - \alpha_n x_0 J_{0n0}] = 0 \quad \text{(A.10)}$$

$$J_{1m1}[2Y_{1m0} - \alpha_m x_0 Y_{0mo}] - Y_{1m1}[2J_{1m0} - \alpha_m x_0 J_{0m0}] = 0 \quad \text{(A.11)}$$

b. When $m = n$, one needs the following identities,

$$J_{1mi}Y_{0mi} - J_{0mi}Y_{1mi} = \frac{2}{\pi\alpha_m x_i} \quad \text{(A.12)}$$

i can be 0 or 1. With integrals in Eq. (A.4) and Eqs. (A.11-12), it can be shown that,

$$2\alpha_m^2 \int_{x_0}^{x_1} xU_m(x)U_m(x)dx$$

$$= \langle J_{1m1}^2 z^2[Y_1^2(z) + Y_0^2(z)] - 2J_{1m1}^2 zY_0(z)Y_1(z)$$

$$-2J_{1m1}Y_{1m1}\{z^2[J_0(z)Y_0(z) + J_1(z)Y_1(z)] - 2zJ_1(z)Y_0(z)\}$$

$$+Y_{1m1}^2 z^2[J_1^2(z) + J_0^2(z)] - 2Y_{1m1}^2 zJ_0(z)J_1(z)\rangle|_{\alpha_m x_0}^{\alpha_m x_1}$$

$$= \frac{4}{\pi^2} - (\alpha_m x_0)^2\Delta^2 \quad \text{(A.13)}$$

where $\Delta = J_{1m1}Y_{1m0} - Y_{1m1}J_{1m0}$.

A.4 Integration

In order to determine the coefficients of C_m, one has to work out the following integration,

$$\alpha_m^2 \int_{x_0}^{x_1} \left(1 - \frac{x}{x_1}\right) x U_m(x) dx$$

$$= \int_{\alpha_m x_0}^{\alpha_m x_1} z[J_{1m1} Y_1(z) - Y_{1m1} J_1(z)] dz - \frac{1}{x_1 \alpha_m} \int_{\alpha_m x_0}^{\alpha_m x_1} z^2 [J_{1m1} Y_1(z) - Y_{1m1} J_1(z)] dz$$

With integrals in Eqs. (A.6-7) and Eqs. (A.11-12), one can find,

$$\alpha_m^2 \int_{x_0}^{x_1} \left(1 - \frac{x}{x_1}\right) x U_m(x) dx = -H_{1m1} + \frac{\pi}{2}(2H_{1m0} - \alpha_m x_0 H_{0m0})\Delta + \frac{2}{\pi} \quad \text{(A.14)}$$

where H_ν are the Struve function of order ν.

Table 1 Values of coefficients β_n with $\tau = 2.5$ and their corresponding Struve function results

No.	$\beta_n = \alpha_n x_0$	$H_0(\beta_n)$	$H_1(\beta_n)$	$H_0(\beta_n \tau)$
1	1.66587424966859	0.76782919939071	0.48821876318662	0.48821876318662
2	3.46654024675250	0.37601360397385	1.08972199199506	1.08972199199506
3	5.44558877655249	-0.22657230036734	0.65110156042030	0.65110156042030
4	7.48347465240147	0.19674126258965	0.38588158606551	0.38588158606551
5	9.54498705593612	0.22794517763496	0.85310481659537	0.85310481659537
6	11.6180079403612	-0.17604478396564	0.67181180541025	0.67181180541025
7	13.6974350624300	0.11741330588462	0.43899940144122	0.43899940144122
8	15.7807779094053	0.17266413295270	0.79431486503444	0.79431486503444
9	17.8666835911315	-0.14927278010559	0.67176218614100	0.67176218614100

Table 2 Values of Bessel functions, Δ functions, and coefficients C_n

No.	$J_1(\beta_n \tau)$	$Y_1(\beta_n \tau)$	$\Delta = U_n(x_0)$	C_n
1	-0.126384182	0.374226728	-0.176713193	2.026829781
2	0.271029369	0.019002595	0.107584365	-0.907938617
3	0.061832572	-0.207444222	-0.071688222	0.64467594
4	-0.145289034	-0.113822135	0.052933135	-0.432981319
5	-0.145734404	0.073876444	-0.041762887	0.358690929
6	0.000267714	0.148081195	0.03442302	-0.280510018
7	0.120807429	0.06326472	-0.029252699	0.247211959
8	0.105293443	-0.071089832	0.025421232	-0.207190957
9	-0.01103938	-0.118884304	-0.022471389	0.188438102

Figures

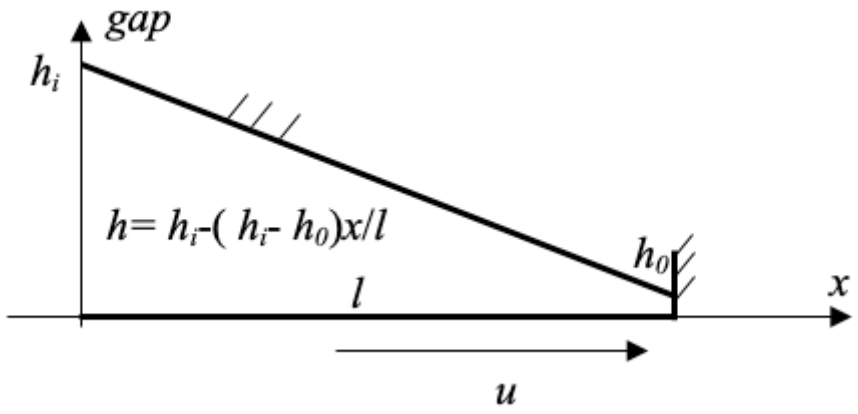

Figure 1

Tilted straight plate, blocked exit

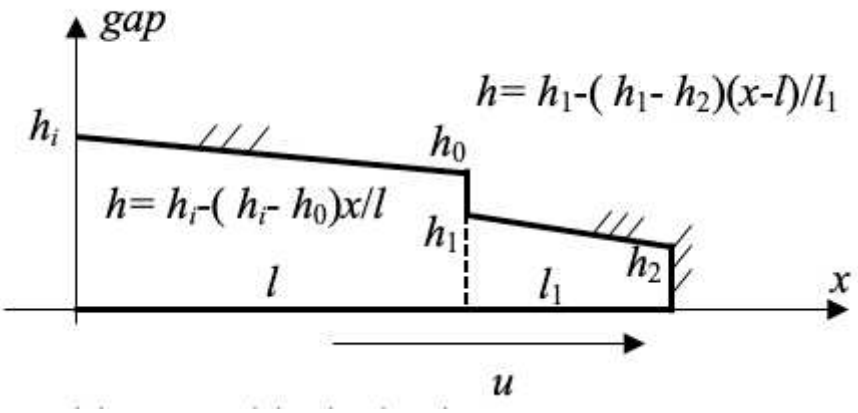

Figure 2

Tilted plate with a step, blocked exit

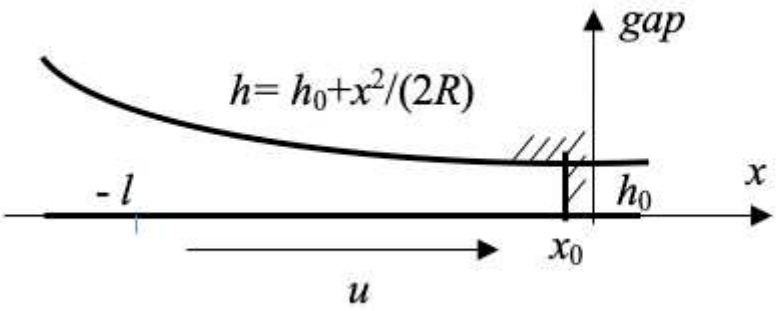

Figure 3

Cylinder, blocked exit

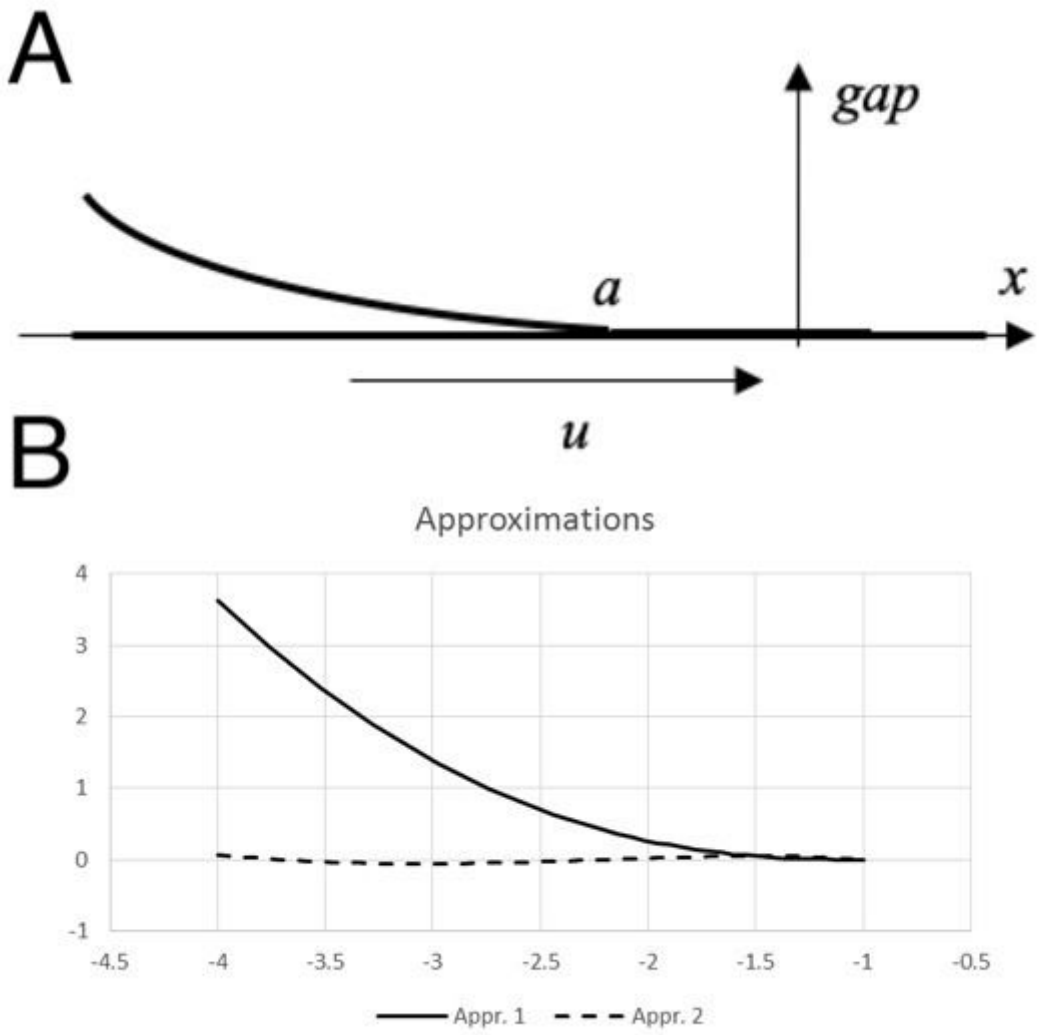

Figure 4

4a Deformed cylinder. 4b Absolute errors from two approximations of 2R h/a2: with exponents of 1.5 (Solid line) and 1.673 (Dashed-line)

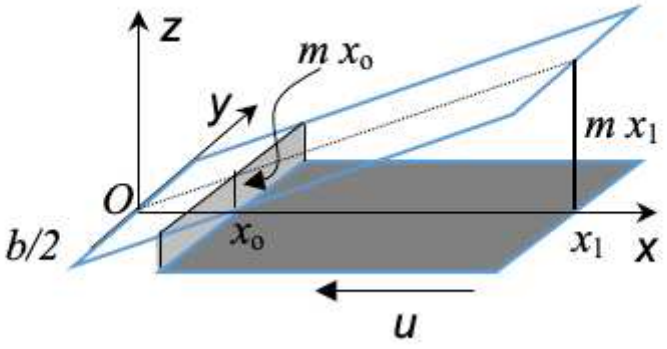

Figure 5

Fixed incline pad bearing, blocked exit

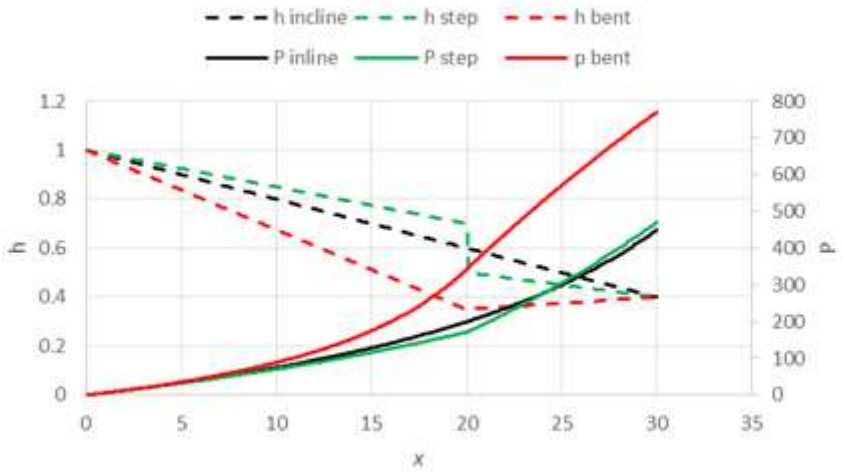

Figure 6

Three plates and their modified pressure

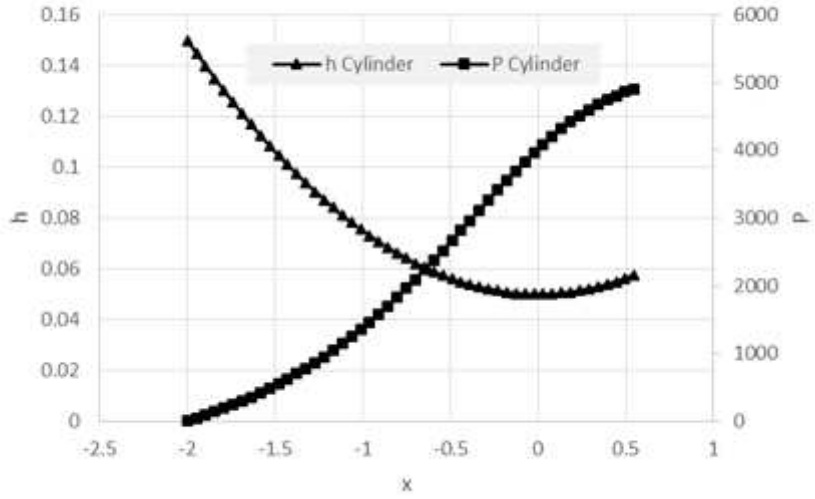

Figure 7

Cylinder and its modified pressure

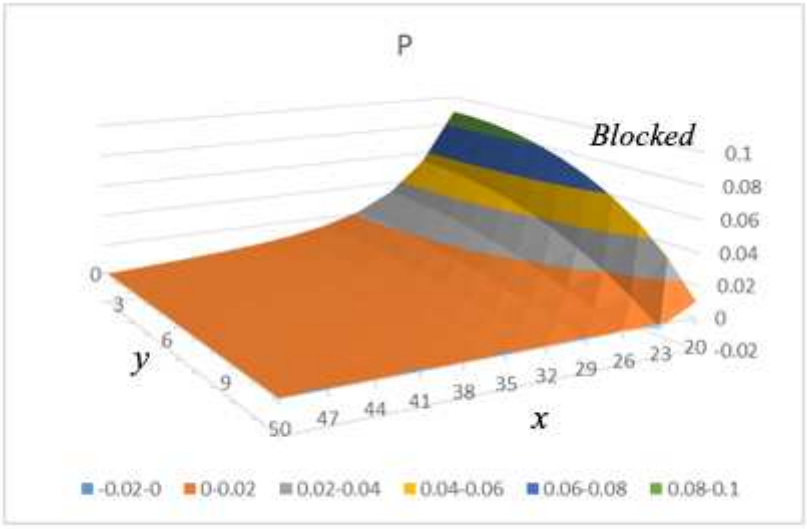

Figure 8

Distribution of the modified pressure shown with y from 0 to 10.

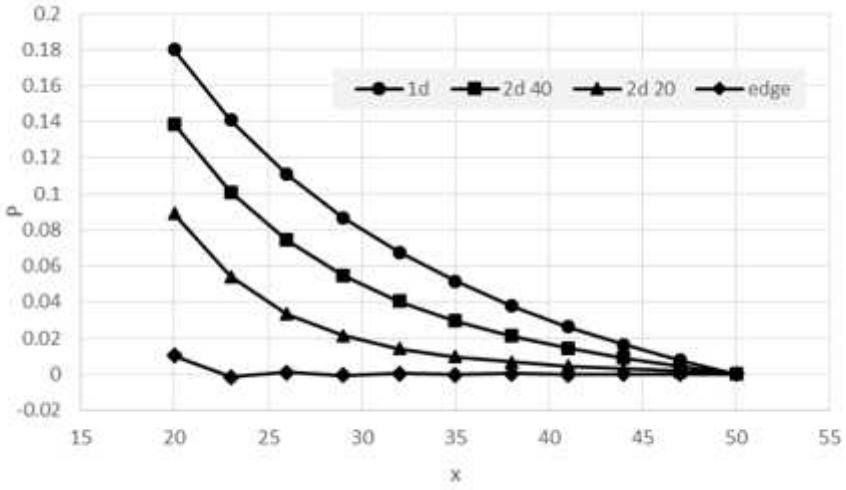

Figure 9

Comparison of modified pressure